

Distribution amplitudes and decay constants for (π, K, ρ, K^*) mesons in light-front quark model

Ho-Meoyng Choi^a and Chueng-Ryong Ji^b

^a Department of Physics, Teachers College, Kyungpook National University, Daegu, Korea 702-701

^b Department of Physics, North Carolina State University, Raleigh, NC 27695-8202

We present a calculation of the quark distribution amplitudes(DAs), the Gegenbauer moments, and decay constants for π, ρ, K and K^* mesons using the light-front quark model. While the quark DA for π is somewhat broader than the asymptotic one, that for ρ meson is very close to the asymptotic one. The quark DAs for K and K^* show asymmetric form due to the flavor $SU(3)$ -symmetry breaking effect. The decay constants for the transversely polarized ρ and K^* mesons(f_ρ^T and $f_{K^*}^T$) as well as the longitudinally polarized ones(f_ρ and f_{K^*}) are also obtained. Our averaged values for f_V^T/f_V , i.e. $(f_\rho^T/f_\rho)_{av} = 0.78$ and $(f_{K^*}^T/f_{K^*})_{av} = 0.84$, are found to be consistent with other model predictions. Especially, our results for the decay constants are in a good agreement with the $SU(6)$ symmetry relation, $f_{\rho(K^*)}^T = (f_{\pi(K)} + f_{\rho(K^*)})/2$.

I. INTRODUCTION

Hadronic distribution amplitudes(DAs) are important ingredients in applying QCD to hard exclusive processes via the factorization theorem [1, 2, 3]. They provide essential information on the nonperturbative structure of hadron describing the distribution of partons in terms of the longitudinal momentum fractions inside the hadron. Both the electromagnetic form factors at high Q^2 and the B -physics phenomenology are highly relevant to the detailed computation of hadronic DAs.

During the past few decades, there have been many theoretical efforts to calculate the pion DA using non-perturbative methods such as the QCD sum rule [3, 4, 5, 6, 7, 8], lattice calculation [9, 10, 11, 12, 13], chiral quark model from the instanton vacuum [14, 15, 16], Nambu-Jona-Lasinio(NJL) model [17, 18], and light-front quark model(LFQM) [19, 20]. It is well known that the shape of the pion quark DA is very important in the predictions of pion electromagnetic form factor in both nonperturbative and perturbative momentum transfer regimes. The QCD sum-rule based analysis [6, 7] of the $\pi - \gamma$ transition form factor $F^{\pi\gamma\gamma^*}(Q^2)$ measured by the CLEO experiment [21] has shown that neither double-humped DA for the pion predicted by Chernyak and Zhitnitsky [3] nor the asymptotic one are favored at the 2σ level of accuracy. It is also interesting to note that the recent anti-de Sitter space geometry/conformal field theory(AdS/CFT) prediction [22] for the meson DA is $\phi_{\text{AdS/CFT}}(x) \propto \sqrt{x(1-x)}$, which would approach to the asymptotic form $x(1-x)$ only in the limit of $\ln Q^2 \rightarrow \infty$. The shape of $\phi_{\text{AdS/CFT}}(x)$ increases the usual perturbative QCD (PQCD) predictions for the pion form factor and $\pi - \gamma$ transition form factor by 16/9 and 4/3, respectively. In our recent LFQM application to the PQCD analysis of the pion form factor [23], we further found a correlation between the shape of quark DA and the amount of soft and hard contributions to the pion form factor. Similar to the previous findings from the Sudakov suppression of the soft contribution (or enhancement of

the hard contribution) [24, 25, 26, 27], our results indicated that the suppression of the endpoint region for the quark DA corresponds to the suppression(enhancement) of the soft(hard) contribution.

Another important area that requires detailed study of meson DAs is the B -physics phenomenology under intense experimental investigation at BaBar and Belle experiments. The K, ρ and K^* DAs have attracted attention rather recently [28, 29, 30, 31] due to the deep relevance to the exclusive B -meson decays to (K, ρ, K^*) mesons. In particular, the $SU(3)$ flavor symmetry breaking effect in the meson quark DA including strange quark is important for the predictions of exclusive $B_{u,d,s}$ -decays to light pseudoscalar and vector mesons in the context of CP-violation and Cabibbo-Kobayashi-Maskawa quark mixing matrix studies. The $SU(3)$ breaking effect is realized in the difference between the longitudinal momenta of the strange and nonstrange quark, $\langle x_s - x_{u(d)} \rangle \neq 0$, in the two particle Fock components of the meson. The similar effect was also found in our PQCD analysis [32] for the exclusive heavy meson pair production in e^+e^- annihilations at $\sqrt{s} = 10.6$ GeV. Not only the shape of the heavy meson quark DAs matters in the prediction of the cross section for the heavy meson pair productions, but also the cross section ratios for $\sigma(e^+e^- \rightarrow D_s^+ D_s^-)/\sigma(e^+e^- \rightarrow D^+ D^-)$ and $\sigma(e^+e^- \rightarrow B_s^0 \bar{B}_s^0)/\sigma(e^+e^- \rightarrow B^+ B^-)$ deviate from 1 appreciably due to the $SU(3)$ symmetry breaking.

A particularly convenient and intuitive framework in applying PQCD to exclusive processes is based upon the light-front(LF) Fock-state decomposition of hadronic state. In the LF framework, the valence quark DA is computed from the valence LF wave function $\Psi_n(x_i, \mathbf{k}_{\perp i})$ of the hadron at equal LF time $\tau = t + z/c$ which is the probability amplitude to find n constituents(quarks, antiquarks, and gluons) with LF momenta $k_i = (x_i, \mathbf{k}_{\perp i})$ in a hadron. Here, x_i and $\mathbf{k}_{\perp i}$ are the LF momentum fraction and the transverse momenta of the i th constituent in the n -particle Fock-state, respectively. If the factorization theorem in PQCD is applicable to exclusive processes, then the invariant amplitude \mathcal{M}

for exclusive process factorizes into the convolution of the process-independent valence quark DA $\phi(x, \mu)$ with the process-dependent hard scattering amplitude T_H [1], i.e.

$$\mathcal{M} = \int [dx_i] \int [dy_i] \phi(x_i, \mu) T_H(x_i, y_i, \mu) \phi(y_i, \mu), \quad (1)$$

where $[dx_i] = \delta(1 - \sum_{k=1}^n x_k) \prod_{k=1}^n dx_k$ and n is the number of quarks in the valence Fock state. Here, μ denotes the separation scale between perturbative and nonperturbative regime. Since the collinear divergences are summed in $\phi(x_i, \mu)$, the hard scattering amplitude T_H can be systematically computed as a perturbative expansion in $\alpha_s(\mu)$. To implement the factorization theorem given by Eq. (1) at high momentum transfer, the hadronic wave function plays an important role linking between long distance nonperturbative QCD encoded in DA and short distance PQCD encoded in T_H .

The quark DA of a meson, $\phi(x, \mu)$, is the probability of finding collinear quarks up to the scale μ in the $L_z = 0$ (s -wave) projection of the meson wave function defined by

$$\phi(x_i, \mu) = \int^{|\mathbf{k}_\perp| < \mu} [d^2 \mathbf{k}_\perp] \Psi(x_i, \mathbf{k}_\perp), \quad (2)$$

where

$$[d^2 \mathbf{k}_\perp] = 2(2\pi)^3 \delta \left[\sum_{j=1}^n \mathbf{k}_{\perp j} \right] \prod_{i=1}^n \frac{d^2 \mathbf{k}_{\perp i}}{2(2\pi)^3}. \quad (3)$$

Simple relativistic quark-model based on the LF framework has been studied for various mesons [19, 20, 33, 34]. Although the proof of duality between the LFQM and the first principle QCD is not yet available, we have attempted to fill the gap between the model wave function and the QCD-motivated effective Hamiltonian [35, 36]. The essential feature of our LFQM [35, 36] is to treat the gaussian radial wave function as a trial function for the variational principle to the QCD-motivated Hamiltonian. We saturate the Fock state expansion by the constituent quark and antiquark, i.e. $H_{q\bar{q}} = H_0 + V_{\text{int}}$, where the interaction potential V_{int} consists of confining and hyperfine interaction terms. From the variational principle minimizing the central Hamiltonian with respect to the gaussian parameter, we can find the optimum values of our model parameters and predict the mass spectra for the low-lying ground state pseudoscalar and vector mesons [35, 36]. We applied our LFQM for various exclusive processes such as the electromagnetic form factors of π , K and ρ [35, 37] mesons and semileptonic and rare B decays to π and K [36, 38]. Our results for the above exclusive processes were in a good agreement with the available data as well as other theoretical model predictions.

The purpose of this work is to calculate the quark DAs, the Gegenbauer moments, and decay constants for π , ρ , K and K^* mesons using our LFQM and compare with other theoretical model predictions. As expected, while the odd Gegenbauer moments for π and ρ meson

DAs are found to be zero due to isospin symmetry, the odd moments for K and K^* meson DAs are nonzero due to the flavor SU(3)-symmetry breaking effect. We compute the decay constants for the transversely polarized ρ and K^* mesons (f_ρ^T and $f_{K^*}^T$) as well as the longitudinally polarized ones (f_ρ and f_{K^*}) and compare with the light-cone sum rule (LCSR) calculations, in which the ratio of f_V^T and f_V is an important ingredient for the LCSR predictions of the $B \rightarrow \rho$ and $B \rightarrow K^*$ transition form factors. We also confirm that our results for the decay constants follow an old SU(6) symmetry relation [39], $f_{\rho(K^*)}^T = (f_{\pi(K)} + f_{\rho(K^*)})/2$.

The paper is organized as follows: In Sec. II, we briefly describe the formulation of our LFQM [35, 36] and the procedure of fixing the model parameters using the variational principle for the QCD-motivated effective Hamiltonian. The shape of the quark DA is then uniquely determined in our model calculation. In Sec. III, the formulae for the quark DAs and decay constants of pseudoscalar and vector mesons are given in our LFQM. The Gegenbauer and ξ ($= x_1 - x_2$) moments are also given in this section. In Sec. IV, we present the numerical results for the decay constants, the quark DAs, the Gegenbauer and ξ moments for (π , K , ρ , K^*) mesons and compare with other theoretical model predictions. Summary and conclusions follow in Sec. V. The relations between ξ and Gegenbauer moments are presented in Appendix A.

II. MODEL DESCRIPTION

In our LFQM [35, 36], the meson wave function is given by

$$\Psi_M^{JJ_z}(x, \mathbf{k}_\perp, \lambda \bar{\lambda}) = \phi_R(x, \mathbf{k}_\perp) \mathcal{R}_{\lambda \bar{\lambda}}^{JJ_z}(x, \mathbf{k}_\perp), \quad (4)$$

where $\phi_R(x, \mathbf{k}_\perp)$ is the radial wave function and $\mathcal{R}_{\lambda \bar{\lambda}}^{JJ_z}(x, \mathbf{k}_\perp)$ is the spin-orbit wave function obtained by the interaction-independent Melosh transformation [40] from the ordinary equal-time static spin-orbit wave function assigned by the quantum numbers J^{PC} . The meson wave function in Eq. (4) is represented by the Lorentz-invariant variables $x_i = p_i^+/P^+$, $\mathbf{k}_{\perp i} = \mathbf{p}_{\perp i} - x_i \mathbf{P}_\perp$ and λ_i , where P , p_i and λ_i are the meson momentum, the momenta and the helicities of the constituent quarks, respectively.

The radial wave function $\phi_R(x, \mathbf{k}_\perp)$ of a ground state pseudoscalar meson ($J^{PC} = 0^{-+}$) is given by

$$\phi_R(x, \mathbf{k}_\perp) = \left(\frac{1}{\pi^{3/2} \beta^3} \right)^{1/2} \exp(-\vec{k}^2/2\beta^2), \quad (5)$$

where $\vec{k}^2 = \mathbf{k}_\perp^2 + k_z^2$ and the gaussian parameter β is related with the size of the meson. Here, the longitudinal component k_z of the three momentum is given by $k_z = (x_1 - \frac{1}{2})M_0 + (m_2^2 - m_1^2)/2M_0$ with the invariant mass

$$M_0^2 = \frac{\mathbf{k}_\perp^2 + m_1^2}{x_1} + \frac{\mathbf{k}_\perp^2 + m_2^2}{x_2}, \quad (6)$$

where $x_1 = x$ and $x_2 = 1 - x$. The covariant form of the spin-orbit wave functions for pseudoscalar($J^{PC} = 0^{-+}$) and vector(1^{--}) mesons are given by

$$\begin{aligned}\mathcal{R}_{\lambda\bar{\lambda}}^{00} &= -\frac{\bar{u}(p_1, \lambda)\gamma_5 v(p_2, \bar{\lambda})}{\sqrt{2}[M_0^2 - (m_1 - m_2)^2]^{1/2}}, \\ \mathcal{R}_{\lambda\bar{\lambda}}^{1J_3} &= -\frac{\bar{u}(p_1, \lambda)\left[\not{\epsilon}(J_z) - \frac{\epsilon \cdot (p_1 - p_2)}{M_0 + m_1 + m_2}\right]v(p_2, \bar{\lambda})}{\sqrt{2}[M_0^2 - (m_1 - m_2)^2]^{1/2}}.\end{aligned}\quad (7)$$

The polarization vectors $\epsilon^\mu = (\epsilon^+, \epsilon^-, \epsilon_\perp)$ used in this analysis are given by

$$\begin{aligned}\epsilon^\mu(\pm 1) &= \left[0, \frac{2}{P^+}\epsilon_\perp(\pm) \cdot \mathbf{P}_\perp, \epsilon_\perp(\pm 1)\right], \\ \epsilon_\perp(\pm 1) &= \mp \frac{(1, \pm i)}{\sqrt{2}}, \\ \epsilon^\mu(0) &= \frac{1}{M_0}\left[P^+, \frac{\mathbf{P}_\perp^2 - M_0^2}{P^+}, \mathbf{P}_\perp\right].\end{aligned}\quad (8)$$

Note that $\sum_{\lambda\bar{\lambda}} R_{\lambda\bar{\lambda}}^{JJ_z\dagger} R_{\lambda\bar{\lambda}}^{JJ_z} = 1$. The normalization of our wave function is given by

$$\begin{aligned}\sum_{\lambda\bar{\lambda}} \int d^3k |\Psi_M^{JJ_z}(x, \mathbf{k}_\perp, \lambda\bar{\lambda})|^2 \\ = \int_0^1 dx \int d^2\mathbf{k}_\perp \left(\frac{\partial k_z}{\partial x}\right) |\phi_R(x, \mathbf{k}_\perp)|^2 = 1,\end{aligned}\quad (9)$$

where the Jacobian of the variable transformation $\{x, \mathbf{k}_\perp\} \rightarrow \vec{k} = (\mathbf{k}_\perp, k_z)$ is given by

$$\frac{\partial k_z}{\partial x} = \frac{M_0}{4x_1x_2} \left\{1 - \left[\frac{(m_1 - m_2)^2}{M_0^2}\right]^2\right\}.\quad (10)$$

The effect of the Jacobi factor has been analyzed in Ref. [41].

The key idea in our LFQM [35, 36] for mesons is to treat the radial wave function $\phi_R(x, \mathbf{k}_\perp)$ as a trial function for the variational principle to the QCD-motivated Hamiltonian saturating the Fock state expansion by the constituent quark and antiquark. The QCD-motivated effective Hamiltonian for a description of the meson mass spectra is given by [42]

$$H_{q\bar{q}} = H_0 + V_{q\bar{q}} = \sqrt{m_q^2 + \vec{k}^2} + \sqrt{m_{\bar{q}}^2 + \vec{k}^2} + V_{q\bar{q}}.\quad (11)$$

In our LFQM [35, 36], we use the two interaction potential $V_{q\bar{q}}$ for the pseudoscalar and vector mesons: (1) Coulomb plus harmonic oscillator(HO), and (2) Coulomb plus linear confining potentials. In addition, the hyperfine interaction, which is essential to distinguish vector from pseudoscalar mesons, is included for both cases, viz.,

$$V_{q\bar{q}} = V_0 + V_{\text{hyp}} = a + \mathcal{V}_{\text{conf}} - \frac{4\kappa}{3r} + \frac{2\mathbf{S}_q \cdot \mathbf{S}_{\bar{q}}}{3m_q m_{\bar{q}}} \nabla^2 V_{\text{Coul}},\quad (12)$$

TABLE I: The constituent quark masses m_q (in GeV) and the gaussian parameters $\beta_{q\bar{q}}$ (in GeV) for the linear[HO] potential obtained from the variational principle. $q=u$ and d .

m_q	m_s	$\beta_{q\bar{q}}$	$\beta_{q\bar{s}}$
0.22[0.25]	0.45[0.48]	0.3659[0.3194]	0.3886[0.3419]

where $\mathcal{V}_{\text{conf}} = br(br^2)$ for the linear(HO) potential and $\langle \mathbf{S}_q \cdot \mathbf{S}_{\bar{q}} \rangle = 1/4(-3/4)$ for the vector(pseudoscalar) meson.

We then take $\phi_R(x, \mathbf{k}_\perp)$ as our trial function to minimize the central Hamiltonian via

$$\frac{\partial \langle \Psi | [H_0 + V_0] | \Psi \rangle}{\partial \beta} = 0.\quad (13)$$

From the above constraint, only 4 parameters are independent among the light-quark masses and the potential parameters $(m_q, \beta_{q\bar{q}}, a, b, \kappa)(q = u, d)$. In order to determine these four parameters from the two experimental values of ρ and π masses, we take the string tension $b = 0.18 \text{ GeV}^2$ and the constituent u and d quark masses $m_u = m_d = 0.22(0.25) \text{ GeV}$ for the linear (HO) potential, which are rather well known from other quark model analyses commensurate with Regge phenomenology [42]. More detailed procedure of determining the model parameters of light quark sector($u(d)$ and s) can be found in [35, 36]. Our model parameters for the light quark sector obtained by the variational principle are summarized in Table I.

III. QUARK DISTRIBUTION AMPLITUDES AND DECAY CONSTANTS

The quark DA of a hadron in our LFQM can be obtained from the hadronic wave function by integrating out the transverse momenta of the quarks in the hadron(see Eq. (2)),

$$\phi(x, \mu) = \int^{|\mathbf{k}_\perp| < \mu} \frac{d^2\mathbf{k}_\perp}{\sqrt{16\pi^3}} \sqrt{\frac{\partial k_z}{\partial x}} \Psi(x, \mathbf{k}_\perp, \lambda\bar{\lambda}).\quad (14)$$

For K and K^* meson cases, we assign the momentum fractions x for s -quark and $(1 - x)$ for the light $u(d)$ -quark. The quark DA describes probability amplitudes to find the hadron in a state with minimum number of Fock constituents and small transverse-momentum separation defined by an ultraviolet(UV) cutoff $\mu \gtrsim 1 \text{ GeV}$. The dependence on the scale μ is then given by the QCD evolution equation[1] and can be calculated perturbatively. However, the DAs at a certain low scale can be obtained by the necessary nonperturbative input from LFQM. Moreover, the presence of the damping Gaussian factor in our LFQM allows us to perform the integral up to infinity without loss of accuracy. The quark DAs for pseudoscalar(P) and vector(V) mesons are constrained by

$$\int_0^1 \phi_{P(V)}(x, \mu) dx = \frac{f_{P(V)}}{2\sqrt{6}},\quad (15)$$

where the decay constant is defined as

$$\langle 0 | \bar{q} \gamma^\mu \gamma_5 q | P \rangle = i f_P P^\mu, \quad (16)$$

for a pseudoscalar meson and

$$\begin{aligned} \langle 0 | \bar{q} \gamma^\mu q | V(P, \lambda) \rangle &= f_V M_V \epsilon^\mu(\lambda), \\ \langle 0 | \bar{q} \sigma^{\mu\nu} q | V(P, \lambda) \rangle &= i f_V^T [\epsilon^\mu(\lambda) P_\nu - \epsilon^\nu(\lambda) P_\mu], \end{aligned} \quad (17)$$

for a vector meson with longitudinal ($\lambda = 0$) and transverse ($\lambda = \pm 1$) polarizations, respectively. The constraint in Eq. (15) must be independent of cut-off μ up to corrections of order Λ^2/μ^2 , where Λ is some typical hadronic scale ($\lesssim 1$ GeV) [1]. For the non-perturbative valence wave function given by Eq. (5), we take $\mu \sim 1$ GeV as an optimal scale for our LFQM.

The explicit form of a pseudoscalar decay constant is given by

$$f_P = \int_0^1 dx \int [d^2 \mathbf{k}_\perp] \frac{\mathcal{A}}{\sqrt{\mathcal{A}^2 + \mathbf{k}_\perp^2}} \phi_R(x, \mathbf{k}_\perp), \quad (18)$$

where $\mathcal{A} = (1-x)m_1 + xm_2$. The decay constants, f_V and f_V^T , for longitudinally and transversely polarized vector mesons, respectively, are given by

$$f_V = \int_0^1 dx \int [d^2 \mathbf{k}_\perp] \frac{\phi_R(x, \mathbf{k}_\perp)}{\sqrt{\mathcal{A}^2 + \mathbf{k}_\perp^2}} \left[\mathcal{A} + \frac{2\mathbf{k}_\perp^2}{M_0 + m_1 + m_2} \right], \quad (19)$$

$$f_V^T = \int_0^1 dx \int [d^2 \mathbf{k}_\perp] \frac{\phi_R(x, \mathbf{k}_\perp)}{\sqrt{\mathcal{A}^2 + \mathbf{k}_\perp^2}} \left[\mathcal{A} + \frac{\mathbf{k}_\perp^2}{M_0 + m_1 + m_2} \right]. \quad (20)$$

The pion decay constant $f_\pi^{\text{exp.}} \simeq 131$ MeV is measured from $\pi \rightarrow \mu\nu$ and the ρ meson decay constant $f_\rho^{\text{exp.}} \simeq 215$ MeV is measured from $\rho \rightarrow e^+e^-$ with the longitudinal polarization. While the constant f_V are known from experiment, the constant f_V^T are not that easily accessible in experiment and hence can be estimated only theoretically.

The average value of the transverse momentum is given by

$$\langle \mathbf{k}_\perp^2 \rangle_{Q\bar{Q}} = \int d^3 k |\mathbf{k}_\perp^2| |\phi_R(x, \mathbf{k}_\perp)|^2. \quad (21)$$

Numerically, we have confirmed that $\langle \mathbf{k}_\perp^2 \rangle_{Q\bar{Q}}^{1/2} = \beta_{Q\bar{Q}}$. This is a nonperturbative measure of the transverse size in the mesonic valence state.

We may also redefine the quark DA as $\Phi_{P(V)}(x) = (2\sqrt{6}/f_{P(V)})\phi(x)$ so that

$$\int_0^1 \Phi_{P(V)}(x) dx = 1. \quad (22)$$

The quark DA $\Phi(x)$ evolved in the leading order (LO) of $\alpha_s(\mu)$ is usually expanded in Gegenbauer polynomials $C_n^{3/2}$ as

$$\Phi(x, \mu) = \Phi_{\text{as}}(x) \left[1 + \sum_{n=1}^{\infty} a_n(\mu) C_n^{3/2}(2x-1) \right], \quad (23)$$

where $\Phi_{\text{as}}(x) = 6x(1-x)$ is the asymptotic DA and the coefficients $a_n(\mu)$ are Gegenbauer moments [1, 17, 43]. The Gegenbauer moments with $n > 0$ describe how much the DAs deviate from the asymptotic one. The zeroth Gegenbauer moment is fixed by the decay constant [1], e.g. for the pion:

$$a_0 = 6 \int_0^1 [dx] \phi_\pi(x_i, \mu) = \frac{3}{\sqrt{6}} f_\pi, \quad (24)$$

where $f_\pi \simeq 131$ MeV. In addition to the Gegenbauer moments, we can also define the expectation value of the longitudinal momentum, so-called ξ -moments:

$$\langle \xi^n \rangle = \int_{-1}^1 d\xi \xi^n \hat{\Phi}(\xi) = \int_0^1 dx \xi^n \Phi(x), \quad (25)$$

where $\Phi(x) = 2\hat{\Phi}(2x-1)$ normalized by $\langle \xi^0 \rangle = 1$. In Appendix A, the relations between $\langle \xi^n \rangle$ and $a_n(\mu)$ are explicitly given up to $n = 6$.

IV. NUMERICAL RESULTS

In our numerical calculations, we use two sets of the model parameters for the linear and harmonic oscillator (HO) confining potentials given in Table I.

We show in Table II our predictions for the decay constants of (π, K, ρ, K^*) mesons and compare with other theoretical model predictions [9, 30] as well as data [45]. As one can see from Table II, our results for the decay constants of (π, K, ρ, K^*) obtained from both linear and HO potential models (especially, those from HO potential) are comparable with the data [45]. Our values for the ratio of f_V^T and f_V , i.e. $f_V^T/f_V = 0.76[0.80]$ and $f_{K^*}^T/f_{K^*} = 0.82[0.86]$ obtained from the linear[HO] potential, are quite comparable with the recent QCD sum rule results, $f_\rho^T/f_\rho = (0.78 \pm 0.08)$ and $f_{K^*}^T/f_{K^*} = (0.78 \pm 0.07)$ [30]. We also find that our results for the decay constants agree surprisingly well with an old SU(6) symmetry relation [39], $f_{\rho(K^*)}^T = (f_{\pi(K)} + f_{\rho(K^*)})/2$ via the sum rule $\phi_{\rho(K^*)}^T = (\phi_{\pi(K)} + \phi_{\rho(K^*)}^L)/2$, where $\phi^{L(T)}(x)$ is the longitudinally(transversely) polarized vector meson DA.

We show in Fig. 1 the normalized quark DAs $\Phi_P(x)$ for π and K mesons obtained from linear(solid line) and HO(dashed line) potentials. For the pion DA, we also compare our results with the asymptotic result $\Phi_{\text{as}}(x) = 6x(1-x)$ (dotted line) as well as the AdS/CFT prediction [22] $\Phi_{\text{AdS/CFT}}(x) = \pi\sqrt{x(1-x)}/8$ (double-dot-dashed line). For the pion case, our quark DAs obtained from both model parameters are somewhat broader than the asymptotic one. We also note from the normalized pion DAs that the suppression of the end point ($x \rightarrow 0$ and 1) region has the following order in DAs, $\Phi_{\text{HO}}(x) > \Phi_{\text{as}}(x) > \Phi_{\text{Linear}}(x) > \Phi_{\text{AdS/CFT}}(x)$. As discussed in Ref. [23], there exists correlation between the shape of nonperturbative quark DA and the amount of low/high

TABLE II: Decay constants(in MeV) for the linear[HO] potential models compared with other models and data.

f_M	Linear[HO]	SR[30]	Lattice[9]	Exp.[45]
f_π	130[131]	-	126.6(6.4)	130.70(10)(36)
f_K	161[155]	-	152.0(6.1)	159.80(1.4)(44)
f_ρ	246[215]	205(9)	239.4(7.3)	220(2) ^(a) , 209(4) ^(b)
f_ρ^T	188[173]	160(10)	-	-
f_{K^*}	256[223]	217(5)	255.5(6.5)	217(5) ^(c)
$f_{K^*}^T$	210[191]	170(10)	-	-

^(a) Exp. value for $\Gamma(\rho^0 \rightarrow e^+e^-)$.

^(b) Exp. value for $\Gamma(\tau \rightarrow \rho\nu_\tau)$.

^(c) Exp. value for $\Gamma(\tau \rightarrow K^*\nu_\tau)$.

Q^2 contributions to the pion form factor. As the end-point region for the quark DA is more suppressed, the soft(hard) contribution to the pion form factor gets suppressed(enhanced). This finding is rather similar to the previous findings from the Sudakov suppression of the soft contribution[24, 25, 26, 27]. For the kaon case, the quark DA is asymmetric due to the flavor SU(3) symmetry breaking effect. The peak points of quark DAs for two potential models are moved slightly to the right of $x = 0.5$ point indicating that s -quark carries more longitudinal momentum fraction than the light $u(d)$ -quark.

In the LO QCD [1], the information of the leading-twist pion DA can be extracted from the pion-photon transition form factor $F_{\pi\gamma}(Q^2)$ as follows:

$$\frac{Q^2 F_{\pi\gamma}^{LO}(Q^2)}{\sqrt{2}f_\pi} \Big|_{\text{twist-2}} = \int_0^1 dx \frac{\Phi_\pi(x, Q)}{6x(1-x)}. \quad (26)$$

The experimental value obtained in CLEO [21] is $Q^2 F_{\pi\gamma}(Q^2) = (16.7 \pm 2.5 \pm 0.4) \times 10^{-2}$ GeV at $Q^2 = 8$ GeV², which goes to $\sqrt{2}f_\pi \simeq 0.185$ GeV in the asymptotic $Q^2 \rightarrow \infty$ limit. With our leading twist pion DA shown in Fig. 1, we obtain $Q^2 F_{\pi\gamma}^{LO}(Q^2) = 0.202[0.181]$ GeV for the linear[HO] potential.

For comparison between the leading twist and next-to-leading twist contributions to $Q^2 F_{\pi\gamma}(Q^2)$, we show in Fig. 2 our previous LFQM [35] prediction for $Q^2 F_{\pi\gamma}(Q^2)$ compared with the data [21, 44]. The thick solid and thick dashed lines represent our linear and HO potential model predictions including the higher twist effects(i.e. \mathbf{k}_\perp and the constituent mass $m = m_u = m_d$) obtained from

$$F_{\pi\gamma}^{NLO}(Q^2) = (e_u^2 - e_d^2) \frac{\sqrt{N_c}}{\pi^{3/2}} \int_0^1 dx \int d^2\mathbf{k}_\perp \sqrt{\frac{\partial k_z}{\partial x}} \times \frac{\phi_R(k^2)}{\sqrt{m^2 + \mathbf{k}_\perp^2}} \frac{(1-x)m}{\mathbf{k}'_\perp{}^2 + m^2}, \quad (27)$$

where N_c is the color factor and $\mathbf{k}'_\perp = \mathbf{k}_\perp + (1-x)\mathbf{q}_\perp$. The thin solid and thin dashed lines represent our leading twist contribution(see Eq. (26)) from $\Phi_{\text{Linear}}(x)$ and $\Phi_{\text{HO}}(x)$, respectively. We also compare our results with the leading twist contributions

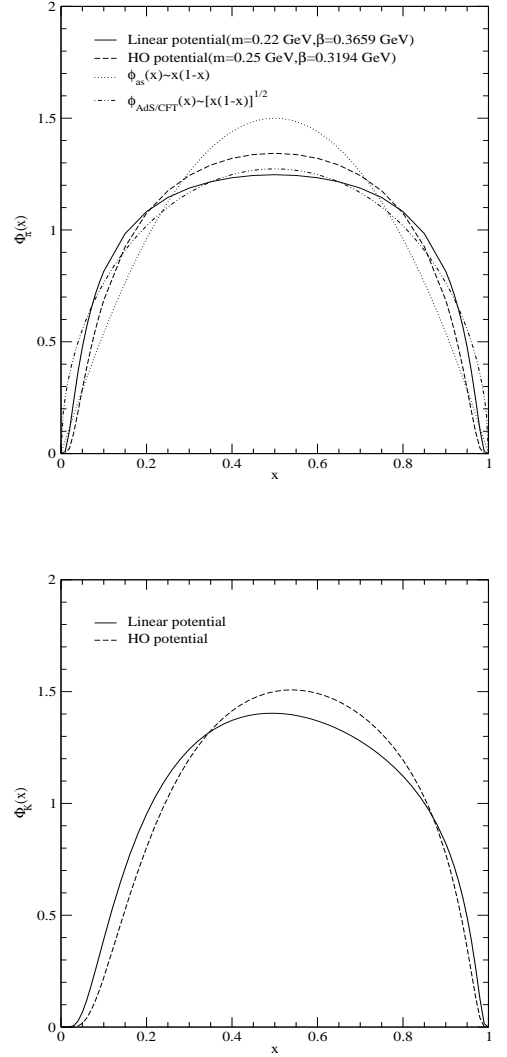


FIG. 1: Normalized DAs $\Phi(x)$ for π and K mesons obtained from linear(solid line) and HO(dashed line) potential models compared with asymptotic result(dotted line) as well as the AdS/CFT prediction [22](double-dot-dashed line).

from the asymptotic $\Phi_{\text{as}}(x)$ (dot-dashed line) and the AdS/CFT $\Phi_{\text{AdS/CFT}}(x)$ (double-dot-dashed line). One should note that the AdS/CFT prediction($\sim \sqrt{x(1-x)}$) increases the usual PQCD prediction($\sim x(1-x)$) by 4/3. Our higher twist results for both potential models are not only very similar to each other but also in good agreement with the experimental data up to $Q^2 \sim 10$ GeV² region. At large Q^2 region, our higher twist prediction for the linear[HO] potential approaches $Q^2 F_{\pi\gamma}^{NLO}(Q^2) = 0.194[0.180]$ compared to the leading twist result 0.202[0.181]. While the higher twist effect on $Q^2 F_{\pi\gamma}(Q^2)$ is large for the low and intermediate Q^2 ($\lesssim 10$ GeV²) region, its effect becomes very small for large Q^2 region compared to the leading twist contribution. Incidentally, it has been found that the leading Fock-state contribution to $F_{\pi\gamma}(Q^2)$ fail to reproduce the $Q^2 = 0$ value corresponding to the axial

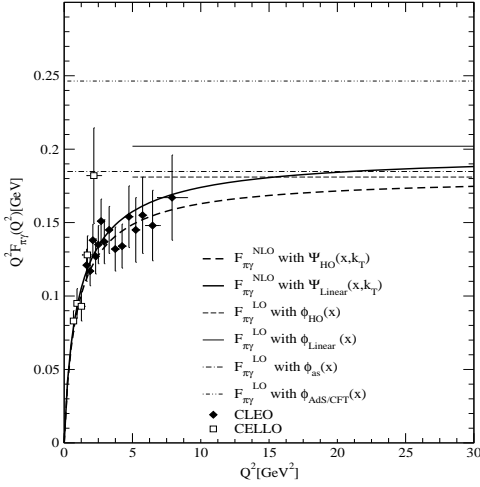


FIG. 2: The leading twist $F_{\pi\gamma}^{LO}(Q^2)$ and the next-to-leading twist $F_{\pi\gamma}^{NLO}(Q^2)$ contributions to $\pi-\gamma$ transition form factor. Data are taken from Refs. [21, 44].

anomaly [47, 48], i.e. it gives only a half of what is needed to get the correct $\pi^0 \rightarrow \gamma\gamma$ rate [49]. However, as shown in Refs. [50, 51, 52], the leading Fock-state contribution to $F_{\pi\gamma}(Q^2)$ has been enhanced by replacing the leading Fock-state wave function to an ‘effective’ valence quark wave function that is normalized to one. By taking the ‘effective’ pion wave function with the asymptotic-like DAs, the authors in [50, 51, 52] found an agreement with the experimental data. Our LFQM prediction [35] also uses the same approach as Refs. [50, 51, 52], i.e. the leading Fock-state ‘effective’ wave function that is normalized to one. The reason why our model is so successful for $F_{\pi\gamma}$ transition form factor is because the Q^2 dependence ($\sim 1/Q^2$) is due to the off-shell quark propagator in the one-loop diagram and there is no angular condition [53] associated with the pseudoscalar meson.

In Tables III and IV, we list the calculated $\langle \xi^n \rangle$ and Gegenbauer moments $a_n(\mu)$ for the pion (Table III) and the kaon (Table IV) DAs obtained from the linear[HO] potential models at the scale $\mu \sim 1$ GeV. We also present the comparison with other model estimates at the scale of $1 \leq \mu \leq 3$ GeV. While the odd Gegenbauer moments of the π meson DA become zero due to isospin symmetry, the odd moments for the kaon are nonzero due to a flavor-SU(3) violation effect of $O(m_s - m_{u(d)})$. For the pion case, our result for the second Gegenbauer moment, $a_2^\pi = 0.12[0.05]$ obtained from linear[HO] potential is quite comparable with other theoretical model predictions given in Table III. A fair average is, however, $a_2^\pi = 0.17 \pm 0.15$ with still large errors [11]. The LCSR based CLEO-data analysis [5, 6, 7] on the transition form factor $F_{\pi\gamma}$ suggests a negative value for a_4^π , which is consistent with the result $a_4^\pi(1\text{GeV}^2) > -0.07$ obtained in Ref. [4]. Our result $a_4^\pi = -0.003[-0.03]$ obtained from the linear[HO] potential also prefers a negative value consistent with the recent LCSR based

CLEO-data analysis [5, 6, 7]. For the kaon case, the first moment is proportional to the difference between the longitudinal momenta of the strange and nonstrange quark in the two-particle Fock component of the kaon, i.e. $a_1^K = (5/3)\langle x_s - x_{\bar{u}} \rangle$ ($x_s = x, x_{\bar{u}} = 1 - x$). The knowledge of a_1^K is important for predicting SU(3)-violation effects within any QCD approach that employs the quark DAs of mesons. In our model calculation, we obtain a positive value of $a_1^K = 0.09[0.13]$ for the linear[HO] potential. Our results for a_1^K are quite consistent with those obtained from other estimates such as the previous LFQM [20] ($a_1^K = 0.08$), the chiral-quark model [15] ($a_1^K = 0.096$) and the QCD sum-rules [28, 29] ($a_1^K = 0.05 \pm 0.02$). The positive sign of a_1^K can be understood intuitively since the heavier strange quark(antiquark) carries a larger longitudinal momentum fraction than the lighter nonstrange antiquark(quark). It is interesting to note that a_1^K for the HO potential model is greater than that for the linear one although the constituent mass difference $m_s - m_u = 0.23$ GeV is the same for both models. This difference is attributed to the fact that the strange quark mass for HO potential model ($m_s = 0.48$ GeV) is larger than for the linear one ($m_s = 0.45$ GeV) and leads to more asymmetric shape for the HO potential. For the second Gegenbauer moment a_2^K , however, the linear potential model gives positive value (0.03), while the HO one gives negative value (-0.03). We note that the QCD sum-rules [28, 29] and lattice calculation [11] give positive values while the chiral quark model [15] gives a negative value.

We show in Fig. 3 the normalized quark DAs for π (upper panel) and K (lower panel) mesons obtained from the linear potential model (exact solution) and compare with those from the truncated Gegenbauer polynomials up to $n = 6$ (approximate solution). For the pion case, the truncation up to $n = 4$ (dashed line) seems more close to our exact solution (solid line) than the truncation up to $n = 6$ (dot-dashed line) although the end-point behavior of $n = 6$ case is more close to the exact solution than $n \leq 4$ case. Since the result up to $n = 2$ truncation is not much different from that up to $n = 4$ truncation, we do not show the result for $n = 2$ case in the figure. For the kaon case, while both truncations up to $n = 4$ (dashed line) and $n = 6$ (dot-dashed line) show good agreement with the exact solution (solid line), the truncation up to $n = 2$ (dotted line) deviates a lot from the exact solution. Thus, it seems not sufficient to truncate the Gegenbauer polynomials only up to $n = 2$ for the kaon case. In both cases of π and K mesons, our model calculation shows that the truncation of the Gegenbauer polynomials up to $n = 4$ seems to give a reasonable approximation to the exact solution.

We show in Fig. 4 the normalized quark DAs $\Phi_\rho(x)$ for the longitudinally (solid line) and transversely (dashed line) polarized ρ meson obtained from the linear (upper panel) and HO (lower panel) potential models and compare with the asymptotic result (dotted line). For both potential models, the quark DA Φ_ρ^L with longitudinal

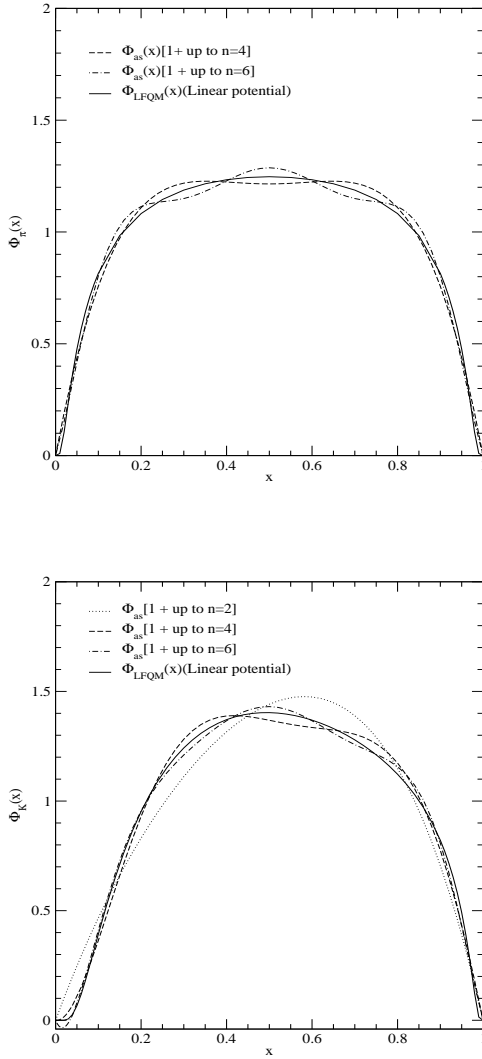


FIG. 3: Normalized DAs for π (upper panel) and K (lower panel) mesons obtained from linear potential model compared with those obtained from the truncated Gegenbauer polynomials up to $n = 6$.

polarization is not much different from the asymptotic result and the quark DA Φ_ρ^T with transverse polarization is somewhat broader than both Φ_ρ^L and Φ_{as} . Overall, the quark DAs for the ρ meson are closer to the asymptotic result than those for the pion case. Although the overall shapes of our Φ_ρ^L and Φ_ρ^T are not much different from the asymptotic result, the end-point behaviors of our model calculation exhibiting the concave shape are different from the asymptotic result of the convex shape. We also should note that our DAs for the ρ meson satisfy the SU(6) symmetry relation [39], $\Phi_\rho^T = (\Phi_\pi + \Phi_\rho^L)/2$.

In Table V, we list the calculated $\langle \xi^n \rangle$ and Gegenbauer moments $a_n(\mu)$ for the ρ meson DAs obtained from the linear[HO] potential models at $\mu \sim 1$ GeV and compare with other model estimates. The odd Gegenbauer moments of both longitudinally and transversely polarized ρ meson DAs become zero due to isospin sym-

metry. Our ξ moments obtained from both linear and HO potential models are similar to the asymptotic results and quite consistent with the previous LFQM [20] and QCD sum-rules [30]. However, slight differences of ξ moments among different model predictions turn out to be quite sensitive in terms of Gegenbauer moments. For instance, the second Gegenbauer moment a_{2L}^ρ for the longitudinally polarized ρ meson obtained from the linear potential model gives positive value(0.02), while the same from the HO potential model gives negative value(-0.02). This may be still comparable with the previous LFQM [20] giving negative value(-0.03) and the QCD sum-rules [30] giving positive value($0.09^{+0.10}_{-0.07}$). Our results for the higher Gegenbauer moments a_n^ρ ($n \geq 4$) obtained from both linear and HO potential models show negative values regardless of polarization states. These negative values for the higher Gegenbauer moments are related with the concave shapes of quark DAs, $\Phi_\rho^L(x)$ and $\Phi_\rho^T(x)$, at the end-point region.

We show in Fig. 5 the normalized quark DAs $\Phi_{K^*}(x)$ for longitudinally(solid line) and transversely(dashed line) polarized K^* meson obtained from the linear(upper panel) and HO(lower panel) potential models. As in the case of the ρ meson, the shape of $\Phi_{K^*}^T$ for the transversely polarized K^* meson near the central($x = 1/2$) region is somewhat broader than that of $\Phi_{K^*}^L$ for the longitudinally polarized K^* meson in both linear and HO models. Also, the peak points for both $\Phi_{K^*}^L$ and $\Phi_{K^*}^T$ are shifted to the right of $x = 1/2$ point due to the SU(3) flavor symmetry breaking as in the case of K meson. Our quark DAs for the K^* meson satisfy also the SU(6) symmetry relation [39], $\Phi_{K^*}^T = (\Phi_K + \Phi_{K^*}^L)/2$.

In Tables VI and VII, we list the calculated $\langle \xi^n \rangle$ and Gegenbauer moments $a_n(\mu)$ for the longitudinally(Table VI) and transversely(Table VII) polarized K^* meson DAs obtained from the linear[HO] potential models at $\mu \sim 1$ GeV and compare with the available QCD sum-rule results [30, 31]. While the odd Gegenbauer moments of the ρ meson DAs become zero due to the isospin symmetry, the odd moments for the K^* meson DAs are nonzero because the SU(3) flavor symmetry is broken. Our values of the first Gegenbauer moments, $a_{1L}^{K^*} = 0.11[0.14]$ and $a_{1T}^{K^*} = 0.10[0.14]$ for the linear[HO] potential model are in a good agreement with the QCD sum-rule results [30] $a_{1L}^{K^*} = a_{1T}^{K^*} = 0.10 \pm 0.07$ at the scale $\mu = 1$ GeV. Note that the positive $a_{1L}^{K^*}$ refers to K^* containing an s quark but the sign will change for \bar{K}^* with an \bar{s} quark. Our predictions for the even powers of $a_{2nL}^{K^*}$ and $a_{2nT}^{K^*}$ ($n \geq 1$) give negative values while the LCSR results [30] give positive values. However, the recent QCD sum-rule result $a_{3T}^{K^*} = 0.02 \pm 0.02$ [31] at the scale $\mu = 1$ GeV is consistent with our value $a_{3T}^{K^*} = 0.04[0.03]$ obtained from the linear[HO] potential model. Also, the $\langle \xi^{2n} \rangle$ moments are not much different between the two models. We show in Fig. 6 the normalized quark DAs for transversely polarized ρ (upper panel) and K^* (lower panel) mesons obtained from the linear potential model and compare with those from the truncated Gegenbauer

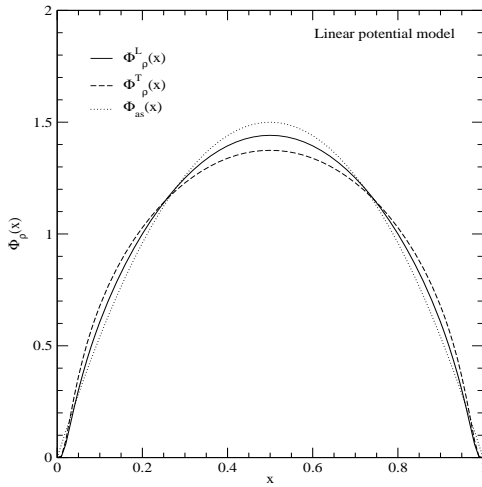


FIG. 4: Normalized DAs for the longitudinally (solid line) and transversely (dashed line) polarized ρ meson obtained from linear (upper panel) and HO (lower panel) potential models compared with asymptotic result (dotted line).

polynomials up to $n = 6$. For the ρ meson case (upper panel), since the truncation up to $n = 2$ does not much differ from that up to $n = 4$ (dashed line), we do not show the result for $n = 2$ case in the figure. Both truncations up to $n = 2$ and $n = 4$ are quite close to our exact solution (solid line). The truncation up to $n = 6$ (dot-dashed line) having a deep at $x = 1/2$ point shows a slight deviation from the exact solution. For the K^* meson case (lower panel), both truncations up to $n = 4$ and $n = 6$ show good agreement with the exact solution, while the truncation up to $n = 2$ (dotted line) deviates a lot from the exact solution. For both ρ and K^* meson cases, the truncation of the Gegenbauer polynomials up to $n = 4$ seems to give an overall reasonable approximation to the exact solution.

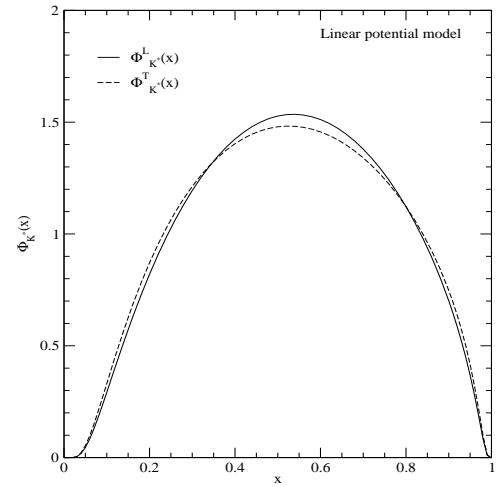


FIG. 5: Normalized DAs for longitudinally (solid line) and transversely (dashed line) polarized K^* meson obtained from linear (upper panel) and HO (lower panel) potential models, respectively.

V. SUMMARY AND DISCUSSION

In this work, we investigated the quark DAs, the Gegenbauer moments, and decay constants for π , ρ , K and K^* mesons using the LFQM constrained by the variational principle for the QCD-motivated effective Hamiltonian. Our model parameters obtained from the variational principle uniquely determine the above nonperturbative quantities.

Our predictions for the quark DAs for π and ρ mesons show somewhat broader shapes than the asymptotic one. The odd Gegenbauer moments for π and ρ meson DAs become zero due to isospin symmetry. Our predictions for a_2^π and a_4^π are consistent with the recent light-cone sum-rule based CLEO data analysis for the pion-photon transition form factor. Interestingly, we also find that our leading twist result for the pion-photon tran-

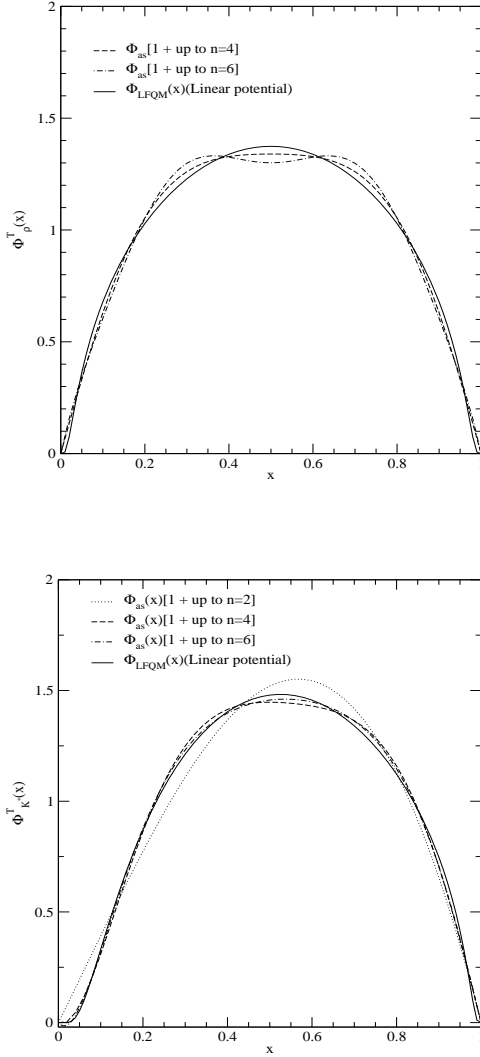


FIG. 6: Normalized DAs for the transversely polarized ρ (upper panel) and K^* (lower panel) mesons obtained from linear potential model compared with those obtained from Gegenbauer polynomials up to $n = 6$.

sition form factor, $Q^2 F_{\pi\gamma}^{LO}(Q^2) = 0.202[0.181]$ GeV obtained from the linear[HO] potential model, is reduced to $Q^2 F_{\pi\gamma}^{NLO}(Q^2) = 0.194[0.180]$ if we include the higher twist effects such as the transverse momentum and the constituent mass. Our result is quite compatible with the CLEO data, $Q^2 F_{\pi\gamma}(Q^2) = (16.7 \pm 2.5 \pm 0.4) \times 10^{-2}$ GeV at $Q^2 = 8$ GeV² [21]. The quark DAs for K and K^* show asymmetric forms due to the flavor SU(3)-symmetry breaking effect. This leads to the nonzero values of the odd Gegenbauer moments. In our model calculations of the quark DAs for (π, K, ρ, K^*) mesons, the truncation of the Gegenbauer polynomials up to $n = 4$ seems to give a reasonable approximation to the exact solution.

Our predictions for the decay constants for π , K , longitudinally polarized ρ and K^* mesons are in a good agreement with the data. We also obtain the decay constants

for the transversely polarized ρ and K^* mesons (f_ρ^T and $f_{K^*}^T$) using our LFQM. Our predicted values of f_V^T/f_V averaged between the linear and HO potential cases are $(f_\rho^T/f_\rho)_{av} = 0.78$ and $(f_{K^*}^T/f_{K^*})_{av} = 0.84$. They are consistent with the recent QCD sum rule results, $f_\rho^T/f_\rho = (0.78 \pm 0.08)$ and $f_{K^*}^T/f_{K^*} = (0.78 \pm 0.07)$ [30]. Moreover, our results for the decay constants are in a good agreement with the SU(6) symmetry relation [39], $f_{\rho(K^*)}^T = (f_{\pi(K)} + f_{\rho(K^*)})/2$ via the sum rule $\phi_{\rho(K^*)}^T = (\phi_{\pi(K)} + \phi_{\rho(K^*)})/2$. Further investigations to utilize our LFQM are underway.

Acknowledgments

This work was supported by a grant from the U.S. Department of Energy under Contract No. DE-FG02-03ER41260. H.-M. Choi was supported in part by Korea Research Foundation under the contract KRF-2005-070-C00039. This research also used resources of the National Energy Research Scientific Computing Center, which is supported by the Office of Science of the U.S. Department of Energy under Contract No. DE-AC02-05CH11231.

APPENDIX A: RELATION BETWEEN ξ AND GEGENBAUER MOMENTS

The ξ -moments $\langle \xi^n \rangle$ defined by Eq.(25) can be related to the Gegenbauer moments $a_n(\mu)$ in Eq.(23). The relations up to $n = 6$ are given by

$$\begin{aligned} \langle \xi^1 \rangle &= \frac{3}{5} a_1, \\ \langle \xi^2 \rangle &= \frac{12}{35} a_2 + \frac{1}{5}, \\ \langle \xi^3 \rangle &= \frac{9}{35} a_1 + \frac{4}{21} a_3, \\ \langle \xi^4 \rangle &= \frac{3}{35} + \frac{8}{35} a_2 + \frac{8}{77} a_4, \\ \langle \xi^5 \rangle &= \frac{1}{7} a_1 + \frac{40}{231} a_3 + \frac{8}{143} a_5, \\ \langle \xi^6 \rangle &= \frac{1}{21} + \frac{12}{77} a_2 + \frac{120}{1001} a_4 + \frac{64}{2145} a_6. \end{aligned} \quad (A1)$$

Also, the first six Gegenbauer polynomials in Eq.(23) are as follows:

$$\begin{aligned} C_1^{3/2}(\xi) &= 3\xi, \\ C_2^{3/2}(\xi) &= \frac{3}{2}(5\xi^2 - 1), \\ C_3^{3/2}(\xi) &= \frac{5}{2}\xi(7\xi^2 - 3), \\ C_4^{3/2}(\xi) &= \frac{15}{8}(21\xi^4 - 14\xi^2 + 1), \\ C_5^{3/2}(\xi) &= \frac{21}{8}\xi(33\xi^4 - 30\xi^2 + 5), \\ C_6^{3/2}(\xi) &= \frac{1}{16}(3003\xi^6 - 3465\xi^4 + 945\xi^2 - 35). \end{aligned} \quad (A2)$$

-
- [1] G. P. Lepage and S. J. Brodsky, Phys. Rev. D **22**, 2157 (1980); S.J. Brodsky, T. Huang, and G.P. Lepage, in *Particles and Fields-2*, Proceedings of the Banff Summer Institute, Banff, Alberta, 1981, edited by A.Z.Capri and A.N. Kamal(Plenum, New York, 1983), p. 143.
- [2] A.V. Efremov and A.V. Radyushkin, Phys. Lett. B **94**, 245 (1980).
- [3] V.L. Chernyak and A.R. Zhitnitsky, Phys. Rep. **112**, 173 (1984).
- [4] P. Ball and R. Zwicky, Phys. Lett. B **625**, 225 (2005).
- [5] S.S. Agaev, Phys. Rev. D **72**, 114010 (2005).
- [6] A. Schmedding and O. Yakovlev, Phys. Rev. D **62**, 116002 (2000).
- [7] A.P. Bakulev, S.V. Mikhailov, and N.G.Stefanis, Phys. Rev. D **73**, 056002 (2006).
- [8] A.P. Bakulev, S.V. Mikhailov, and N.G.Stefanis, Phys. Lett. B **508**, 279 (2001); **590(E)**, 309 (2004).
- [9] A. Ali Khan, et al., Phys. Rev. D **64**, 054504 (2001); Phys. Rev. D **65**, 054505 (2002).
- [10] S. Dalley and B. van de Sande, Phys. Rev. D **67**, 114507 (2003).
- [11] V. M. Braun *et al.*[QCDSF/UKQCD Collaboration], Phys. Rev. D **74**, 074501 (2006).
- [12] M.Göckeler *et al.*, hep-lat/0510089.
- [13] L. Del Debbio, Few-Body Syst., Suppl. **36**, 77 (2005).
- [14] V.Y. Petrov, M. V.Polyakov, R.Ruskov, C. Weiss, and K. Goeke, Phys. Rev. D **59**, 114018 (1999).
- [15] S.I. Nam, H.-C. Kim, A. Hosaka, and M.M. Musakhanov, Phys. Rev. D **74**, 014019 (2006).
- [16] I.V. Anikin, A.E. Dorokhov, and L. Tomio, Phys. Atom. Nucl. **64**, 1405 (2001).
- [17] E. R. Arriola and W. Broniowski, Phys. Rev. D **66**, 094016 (2002).
- [18] M. Praszalowicz and A. Rostworowski, Phys. Rev. D **64**, 074003 (2001); Phys. Rev. D **66**, 054002 (2002).
- [19] C.-R.Ji and S.R. Cotanch, Phys. Rev. D **41**, 2319 (1990).
- [20] C.-R. Ji, P.L. Chung, and S.R. Cotanch, Phys. Rev. D **45**, 4214 (1992).
- [21] J. Gronberg *et al.*[CLEO Collaboration], Phys. Rev. D **57**, 33 (1998).
- [22] S. J. Brodsky and G. F. de Teramond, Phys. Lett. B **582**, 211 (2004); Phys. Rev. Lett. **96**, 201601 (2006); G. F. de Teramond and S. J. Brodsky, Phys. Rev. Lett. **94**, 201601 (2005).
- [23] H.-M. Choi and C.-R. Ji, Phys. Rev. D **74**, 093010 (2006).
- [24] H. N. Li and G. Sterman, Nucl. Phys. B **381**, 129 (1992); H. N. Li, Phys. Rev. D **48**, 4243 (1993).
- [25] O.C. Jacob and L.S. Kisslinger, Phys. Rev. Lett. **56**, 225 (1986); Phys. Lett. B **243**, 323 (1990).
- [26] R. Jakob and P. Kroll, Phys. Lett. B **315**, 463 (1993).
- [27] I.V. Anikin, A.E. Dorokhov, and L. Tomio, Phys. Lett. B **475**, 361 (2000); A.E. Dorokhov, JETP Lett. **77**, 63(2003).
- [28] A. Khodjamirian, Th. Mannel, and M. Melcher, Phys. Rev. D **70**, 094002 (2004).
- [29] P. Ball, V.M. Braun, and A. Lenz, JHEP **0605**, 004 (2006)[hep-ph/0603063].
- [30] P. Ball and R. Zwicky, Phys. Rev. D **71**, 014029 (2005).
- [31] K.C. Yang, JHEP **0510**, 108 (2005).
- [32] H.-M. Choi and C.-R. Ji, Phys. Rev. D **73**, 114020 (2006).
- [33] Z. Dziembowski and L. Mankiewicz, Phys. Rev. Lett. **58**, 2175 (1987); Z. Dziembowski, Phys. Rev. D **37**, 2030 (1988); **37**, 768 (1988); **37**, 778 (1988); J. Bienkowska, Z. Dziembowski and H. J. Weber, Phys. Rev. Lett. **59**, 624 (1987); H. J. Weber, Ann. Phys. (N.Y.) **177**, 38 (1987); Phys. Lett. B **209**, 425 (1988).
- [34] M.A.DeWitt, H.-M.Choi and C.-R. Ji, Phys. Rev. D **68**, 054026 (2003).
- [35] H.-M. Choi and C.-R. Ji, Phys. Rev. D **59**, 074015 (1999).
- [36] H.-M. Choi and C.-R. Ji, Phys. Lett. B **460**, 461 (1999).
- [37] H.-M. Choi and C.-R. Ji, Phys. Rev. D **70**, 053015 (2004).
- [38] H.-M. Choi, C.-R. Ji and L.S. Kisslinger, Phys. Rev. D **65**, 074032 (2002).
- [39] H. Leutwyler, Nucl. Phys. B **76**, 413 (1974); S. Malik, *ibid.* **206**, 90(1982).
- [40] H. J. Melosh, Phys. Rev. D **9**, 1095 (1974).
- [41] H.-M. Choi and C.-R. Ji, Phys. Rev. D **56**, 6010 (1997).
- [42] S. Godfrey and N. Isgur, Phys. Rev. D **32**, 189 (1985); S. Godfrey, Phys. Rev. D **33**, 1391 (1986).
- [43] D. Müller, Phys. Rev. D **51**, 3855 (1995).
- [44] CELLO collaboration, H.-J. Behrend et al., Z. Phys. C **49**, 401 (1991).
- [45] Particle Data Group, S. Eidelman, et al., Phys. Lett. B **592**, 1 (2004).
- [46] E. M. Aitala *et al.*[E791 Collaboration], Phys. Rev. Lett. **86**, 4768 (2001).
- [47] R. Jakob et al., J. Phys. G **22**, 45 (1996); P. Kroll and M. Raulfs, Phys. Lett. B **387**, 848 (1996);
- [48] T. Huang and X.-G. Wu, hep-ph/0606135.
- [49] S. Treiman, R. Jackiw and D. Gross, *Lectures on the Current Algebra and its Applications*, Princeton University Press(Princeton, 1972).
- [50] B.-W. Xiao and B.-Q. Ma, Phys. Rev. D **68**, 034020 (2003).
- [51] I.V. Musatov and A.V. Radyushkin, Phys. Rev. D **56**, 2713 (1997).
- [52] A. V. Radyushkin, Acta Phys. Polon. B **26**, 2067(1995).
- [53] I. L. Grach and L.A. Kondratyuk, Sov. J. Nucl. Phys. **39**, 198(1984); B.L.G. Bakker and C.-R. Ji, Phys. Rev. D **65**, 073002 (2002); B.L.G. Bakker, H.-M. Choi, and C.-R. Ji, Phys. Rev. D **65**, 116001 (2002).

TABLE III: The ξ and Gegenbauer moments $a_n^\pi(\mu)$ for the pion DAs obtained from the linear[HO] potential models compared with other model estimates. The numbers in the parentheses stand for the scales of the corresponding works.

Models	$\langle \xi^2 \rangle$	$\langle \xi^4 \rangle$	$\langle \xi^6 \rangle$	a_2^π	a_4^π	a_6^π
Linear[HO]	0.24[0.22]	0.11[0.09]	0.07[0.05]	0.12[0.05]	-0.003[-0.03]	-0.02[-0.03]
Asymptotic WF	0.20	0.09	0.05	0	0	0
AdS/CFT [22]	0.25	0.125	0.078	0.146	0.057	0.031
[3](2.4 GeV)	0.35	0.21	-	0.44	0.25	-
[4](1.0 GeV)	0.24	0.11	-	0.115	-0.015	-
[5](1.0 GeV)	0.28	0.13	-	0.23	-0.05	-
[8](1.0 GeV)	0.27	0.12	-	0.20	-0.14	-
[14](1.0 GeV)	0.22	0.10	-	0.046	0.007	-
[15](1.0 GeV)	0.21	0.09	0.05	0.029	-0.046	-0.019
[16](1.0 GeV)	0.22	0.09	-	0.05	-0.04	-
[11](2.0 GeV)	0.269(39)	-	-	0.201(114)	-	-
[6](2.4 GeV)	0.24 \pm 0.01	-	-	0.12 \pm 0.03	-	-
[8](2.4 GeV)	0.25	0.11	-	0.14	-0.08	-
[10](2.4 GeV)	0.23	0.11	-	0.08	0.02	-
[21](2.4 GeV)	0.27	0.11	-	0.19	-0.14	-
[46](2.4 GeV)	0.25	0.12	-	0.16	0.02	-

TABLE IV: The ξ and Gegenbauer moments $a_n^K(\mu)$ for the kaon DAs obtained from the linear[HO] potential models compared with other model estimates. The numbers in the parentheses stand for the scales of the corresponding works.

Models	$\langle \xi^1 \rangle$	$\langle \xi^2 \rangle$	$\langle \xi^3 \rangle$	$\langle \xi^4 \rangle$	$\langle \xi^5 \rangle$	$\langle \xi^6 \rangle$
Linear[HO]	0.06[0.08]	0.21[0.19]	0.03[0.04]	0.09[0.08]	0.02[0.03]	0.05[0.04]
[15](1.0 GeV)	0.057	0.182	0.023	0.070	0.012	0.0345
[20](1.0 GeV)	0.046	0.20	0.025	0.08	0.015	0.04
[29](2.0 GeV)	0.03 \pm 0.01	0.26 \pm 0.04	-	-	-	-

Models	a_1^K	a_2^K	a_3^K	a_4^K	a_5^K	a_6^K
Linear[HO]	0.09[0.13]	0.03[-0.03]	0.06[0.04]	-0.02[-0.03]	0.007[-0.01]	-0.01[-0.01]
[15](1.0 GeV)	0.096	-0.051	-0.008	-0.040	-0.002	-0.0097
[20](1.0 GeV)	0.08	0	0.03	-0.06	-0.14	-0.03
[28](1.0 GeV)	0.05 \pm 0.02	0.27 $^{+0.37}_{-0.12}$	-	-	-	-
[11](2.0 GeV)	0.0453(9)(29)	0.175(18)(47)	-	-	-	-
[29](2.0 GeV)	0.05 \pm 0.02	0.17 \pm 0.10	-	-	-	-

TABLE V: The ξ and Gegenbauer moments $a_n^\rho(\mu)$ for the ρ meson DAs obtained from the linear[HO] potential models compared with other model estimates. The numbers in the parentheses stand for the scales of the corresponding works.

Models	$\langle \xi^2 \rangle_L$	$\langle \xi^4 \rangle_L$	$\langle \xi^6 \rangle_L$	$\langle \xi^2 \rangle_T$	$\langle \xi^4 \rangle_T$	$\langle \xi^6 \rangle_T$
Linear[HO]	0.21[0.19]	0.09[0.08]	0.05[0.04]	0.22[0.20]	0.10[0.09]	0.06[0.04]
Asymptotic WF	0.20	0.09	0.05	0.20	0.09	0.05
[20](1.0 GeV)	0.19	0.07	0.036	0.2	0.082	0.042
[30](1.0 GeV)	0.23 $^{+0.03}_{-0.02}$	0.11 $^{+0.03}_{-0.02}$	-	0.23 $^{+0.03}_{-0.02}$	0.11 $^{+0.03}_{-0.02}$	-

Models	a_{2L}^ρ	a_{4L}^ρ	a_{6L}^ρ	a_{2T}^ρ	a_{4T}^ρ	a_{6T}^ρ
Linear[HO]	0.02[-0.02]	-0.01[-0.03]	-0.02[-0.02]	0.06[0.007]	-0.01[-0.03]	-0.02[-0.02]
[20](1.0 GeV)	-0.03	-0.09	0.7	0	-0.04	-0.04
[30](1.0 GeV)	0.09 $^{+0.10}_{-0.07}$	0.03 \pm 0.02	-	0.09 $^{+0.10}_{-0.07}$	0.03 \pm 0.02	-

TABLE VI: The ξ and Gegenbauer moments $a_n^{K^*}(\mu)$ for the longitudinally polarized K^* meson DAs obtained from the linear[HO] potential models compared with other model estimates. The numbers in the parentheses stand for the scales of the corresponding works.

Models	$\langle \xi^1 \rangle_L$	$\langle \xi^2 \rangle_L$	$\langle \xi^3 \rangle_L$	$\langle \xi^4 \rangle_L$	$\langle \xi^5 \rangle_L$	$\langle \xi^6 \rangle_L$
Linear[HO]	0.07[0.09]	0.19[0.18]	0.03[0.04]	0.08[0.07]	0.02[0.02]	0.04[0.03]
[30](1.0 GeV)	0.06 \pm 0.04	0.22 $^{+0.03}_{-0.02}$	-	0.10 \pm 0.02	-	-

Models	$a_{1L}^{K^*}$	$a_{2L}^{K^*}$	$a_{3L}^{K^*}$	$a_{4L}^{K^*}$	$a_{5L}^{K^*}$	$a_{6L}^{K^*}$
Linear[HO]	0.11[0.14]	-0.03[-0.07]	0.03[0.02]	-0.02[-0.03]	0[-0.01]	-0.01[-0.01]
[30](1.0 GeV)	0.10 \pm 0.07	0.07 $^{+0.09}_{-0.07}$	-	0.02 \pm 0.01	-	-

TABLE VII: The ξ and Gegenbauer moments $a_n^{K^*}(\mu)$ for the transversely polarized K^* meson DAs obtained from the linear[HO] potential models and compared with other model estimates. The numbers in the parentheses stand for the scales of the corresponding works.

Models	$\langle \xi^1 \rangle_T$	$\langle \xi^2 \rangle_T$	$\langle \xi^3 \rangle_T$	$\langle \xi^4 \rangle_T$	$\langle \xi^5 \rangle_T$	$\langle \xi^6 \rangle_T$
Linear[HO]	0.06[0.08]	0.20[0.18]	0.03[0.04]	0.08[0.07]	0.02[0.02]	0.04[0.04]
[30](1.0 GeV)	0.06 ± 0.04	$0.22^{+0.03}_{-0.02}$	-	0.10 ± 0.02	-	-
[31](1.0 GeV)	0.06 ± 0.04	-	0.03 ± 0.02	-	-	-
Models	$a_{1T}^{K^*}$	$a_{2T}^{K^*}$	$a_{3T}^{K^*}$	$a_{4T}^{K^*}$	$a_{5T}^{K^*}$	$a_{6T}^{K^*}$
Linear[HO]	0.10[0.14]	-0.008[-0.05]	0.04[0.03]	-0.02[-0.03]	0.003[-0.01]	-0.01[-0.01]
[30](1.0 GeV)	0.10 ± 0.07	$0.07^{+0.09}_{-0.07}$	-	0.02 ± 0.01	-	-
[31](1.0 GeV)	0.10 ± 0.07	-	0.02 ± 0.02	-	-	-